Drug Development and Industrial Pharmacy

ISSN: (Print) (Online) Journal homepage: www.tandfonline.com/journals/iddi20

Ameliorated delivery of amphotericin B to macrophages using chondroitin sulfate surface-modified liposome nanoparticles

Marium Azim, Saeed A. Khan, Nashwa Osman, Sajid K. Sadozai & Iftikhar Khan

To cite this article: Marium Azim, Saeed A. Khan, Nashwa Osman, Sajid K. Sadozai & Iftikhar Khan (22 Dec 2024): Ameliorated delivery of amphotericin B to macrophages using chondroitin sulfate surface-modified liposome nanoparticles, Drug Development and Industrial Pharmacy, DOI: 10.1080/03639045.2024.2443007

To link to this article: https://doi.org/10.1080/03639045.2024.2443007

Published online: 22 Dec 2024.

DRUG DEVELOPMENT AND INDUSTRIAL PHARMACY
https://doi.org/10.1080/03639045.2024.2443007

Taylor & Francis
Taylor & Francis Group

RESEARCH ARTICLE

OPEN ACCESS Check for updates

Ameliorated delivery of amphotericin B to macrophages using chondroitin sulfate surface-modified liposome nanoparticles

Marium Azim[a], Saeed A. Khan[a], Nashwa Osman[b], Sajid K. Sadozai[a] and Iftikhar Khan[b]

[a]Department of Pharmacy, Kohat University of Science and Technology, Kohat, Pakistan; [b]School of Pharmacy and Biomolecular Sciences, Liverpool John Moores University, Liverpool, United Kingdom

ABSTRACT

Background: The neglected tropical disease leishmaniasis has significant adverse effects from current treatments and limited therapeutic options are currently available.

Objective: The aim of this study was to develop a surface-modified nano-liposomal drug delivery system, anchored with chondroitin sulfate (CS), to effectively transport Amphotericin B (AmB) to macrophages.

Methods: Conventional liposome formulations (CL-F) and CS-coated surface-modified liposome formulations (CS-SML-F) were formulated by the thin film hydration method and characterized for particle size, polydispersity index (PDI), zeta potential, and entrapment efficiency with long-term stability. *In-vitro* drug release using simulation medium, deformability index (DI) by using a polycarbonate membrane, and cell uptake studies among murine macrophages *via* flow cytometry were analyzed. Scanning and transmission electron microscopy were used to study the surface morphology and shape of the particles.

Results: Optimized conventional liposome CL-F6, CL-F9 and surface-modified liposomes CS-SML-F6 and CS-SML-F9 exhibited particle size diameters around 280 nm with a PDI of approximately 0.3 over six months of storage at 5 °C, maintaining stable surface charge (circa −30 mV). Sustained drug release peaked between 4 and 12 h and surface morphology showed a uniform distribution of spherical liposome particles. Cell uptake measured by flow cytometry showed the highest rate of macrophage targeting by the CS-SML-Fs.

Conclusion: These findings have demonstrated that CS surface-modification has enhanced nanoparticle targeting to macrophage binding sites, particularly the cysteine-rich domain, potentially advancing macrophage-targeted drug delivery systems.

ARTICLE HISTORY
Received 8 October 2024
Revised 5 December 2024
Accepted 11 December 2024

KEYWORDS
Amphotericin B; liposome; surface-modification; macrophages; leishmaniasis; Leishmania tropica

Introduction

The treatment of leishmaniasis, caused by the protozoan parasite Leishmania, poses significant challenges due to the limitations of conventional therapies and the absence of an effective vaccine. Amphotericin B (AmB), a potent antifungal and anti-leishmanial agent, is ignored by its poor solubility and severe nephrotoxicity, necessitating alternative therapeutic approaches [1]. To address these issues, lipid-based formulations have been developed for parenteral and topical administration to improve AmB therapeutic index. However, the search for safer and more effective treatments persists. Several studies suggested AmB delivery within nanoparticles minimizing cytotoxicity, enhancing therapeutic efficacy and active targeting, offering a potential solution to the challenges posed by current leishmaniasis treatments [2].

Liposomes are considered a milestone in the field of bio-nanotechnology. They were originally discovered by Bangham et al. [3] and they were then developed into many different types and forms [4–7]. Liposomes can be prepared from natural phospholipids, which make them biocompatible and biodegradable and therefore reduce their toxicity. In addition, these carriers possess the ability to encapsulate both hydrophilic (in the central core) and hydrophobic (in concentric bilayers) drugs [8]. AmB-loaded liposomal formulations in combination with CS make them a novel combination targeting leishmaniasis.

CS is a naturally occurring biopolymer that has gained significant interest in the field of drug delivery, particularly for its potential to enhance nanoparticle formulations targeting macrophages for increased drug uptake [9]. Macrophages play a pivotal role in the immune system, acting as key players in the clearance of pathogens and foreign particles. However, traditional drug delivery systems often struggle to effectively target and deliver drugs to macrophages [10]. CS offers a promising solution due to its ability to interact with specific receptors expressed on the surface of macrophages. By modifying nanoparticle surfaces with CS, these nanoparticles can be engineered to specifically target macrophages, thereby enhancing drug uptake efficiency [11]. The mechanism underlying CS-mediated uptake involves the interaction between CS and receptors, such as the mannose receptor (MR) CD206, found on macrophages. This interaction facilitates the internalization of CS-modified nanoparticles by macrophages, leading to improved drug delivery and therapeutic outcomes [10]. Therefore, the utilization of CS in nanoparticle formulation development holds great potential for the advancement of targeted drug delivery systems, particularly in diseases where macrophages play a crucial role in pathogenesis and treatment response [12].

CONTACT Iftikhar Khan I.Khan@ljmu.ac.uk School of Pharmacy and Biomolecular Sciences, Liverpool John Moores University, Liverpool L3 3AF, United Kingdom; Saeed A. Khan saeedkhanphd@gmail.com Department of Pharmacy, Kohat University of Science and Technology, Kohat, Pakistan

Furthermore, the toxicity of pure CS as well as the formulated nanoparticles was found to be negligible, suggesting a promising avenue for safer and more effective treatment strategies [2].

Thus, in this study, novel nanoparticle-based formulations modified with CS for the delivery of AmB were explored, with the goal of achieving improved efficacy and reduced toxicity for the treatment of leishmaniasis.

Materials and methods

Materials

Amphotericin B (85% purity), acetic acid, acetonitrile, methanol, chloroform, and dimethyl sulfoxide (DMSO) were purchased from Fischer Scientific, UK. Dipotassium glycyrrhizinate (KG), chondroitin sulfate sodium (CS), N-Hydroxysuccinamide (NHS), phosphate buffer saline (PBS) tablets, triethanolamine (TA), triton-X100, Nile red (NR) dye, and culture media including RPMI-1640 complete medium with 2 mM L-Glutamine, 10% fetal bovine serum (FBS) and antibiotics (Pen-Strep and Gentamicin)) were obtained from Sigma Aldrich, UK. Polyethylene glycol 400 (PEG400), 1-Ethyl-3-(3-dimethylaminopropyl) carbodiimide (EDC) and octadecylamine (ODA, also known as stearylamine (SA)) were acquired from Thermo Scientific, UK. Polyoxyethylene sorbitan monostearate-61 (Tween61) was acquired from Croda Inc. UK. Soya phosphatidylcholine (SPC; 94% purity) was bought from Lipoid, Steinhaus, Switzerland. J774A.1 monocyte macrophage mouse (ATCC-TIB-67) was purchased from the American Type Cell Culture Collection (ATCC, UK).

Preparation of blank and conventional liposome formulations

Optimization of protocol

In blank liposome formulations (BL-Fs), the surfactant tween61 (100 mg) was dissolved in 10 ml ethanol, and KG in DMSO to prepare a 0.1% w/v solution (0.2 mg in 2 ml DMSO). SPC (100 mg) was dissolved in 10 ml ethanol and KG (10 µL) solutions were added to the surfactant solution and sonicated in a water bath for 5 min at room temperature (RT) to homogenize all the components of the lipid phase in the round bottom flask (RBF). A thin layer was obtained by using a rotary evaporator (RV 8 digital, IKA, UK) under optimized conditions of 40 °C at 150 rpm for 10 min under vacuum. The RBF was removed when the solvent was completely evaporated, and a thin film was formed. It was then hydrated with the aqueous phase (i.e. double distilled water (DDW); 10 ml) containing 26% w/v (2.60 g) PEG400 and kept in a water bath previously adjusted at 40 °C for 15 min for complete thin film hydration. After hydration, the formulation was homogenized through high-pressure homogenization (Ultra Turrax, IKA, UK) at 20,000 rpm for 6 min at RT. Post-homogenization, formulation was probe sonicated (Q125 sonicator, QSONICA, USA) at 40% amplitude for 10 min at RT. Then, each formulation was characterized for particle size (PS), size distribution (also known as polydispersity index (PDI)), zeta potential (ZP), and kept for overnight stability at RT. The rest of the BL-Fs and conventional liposome formulations (CL-Fs) were prepared using various concentrations of formulation ingredients (Table 1).

Table 1. Blank liposome formulations (BL-Fs) without Amphotericin B (AmB), and conventional liposome formulations (CL-Fs) loaded with AmB were prepared with varying concentrations of tween61 and SPC.

Formulations	Tween61% (mg)	SPC (mg)	KG% (µL)	AmB (µg/mL)	PEG400% (mg)	Aqueous phase (mL) / final volume
F1	1, (100)	100	0.1, (10)	500	26, (2600)	10
F2	1.3, (130)	100	0.1, (10)	500	26, (2600)	10
F3	2, (200)	100	0.1, (10)	500	26, (2600)	10
F4	1.3, (130)	160	0.1, (10)	500	26, (2600)	10
F5	4, (400)	160	0.1, (10)	500	26, (2600)	10
F6	3.2, (320)	160	0.1, (10)	500	26, (2600)	10
F7	1, (100)	160	0.1, (10)	500	26, (2600)	10
F8	2, (200)	160	0.1, (10)	500	26, (2600)	10
F9	2.3, (230)	160	0.1, (10)	500	26, (2600)	10
F10	2.3, (230)	100	0.1, (10)	500	26, (2600)	10

Thermodynamic stability study

Overnight stability. All BL-Fs were subjected to overnight stability after preparation. The formulations were placed undisturbed on a benchtop at RT and were observed the next day for any kind of physical instability. Only the stable formulations were selected for the preparation of AmB-loaded conventional liposome formulations (CL-Fs).

Centrifugation test. For further optimization (after overnight stability study), the BL-Fs were subjected to centrifugation at 3500 rpm (1505 rcf) for 30 min at RT. The BL-Fs were observed for any signs of instability.

Heating-cooling cycle. The optimized BL-Fs were subjected to three consecutive heating-cooling cycles. The formulations were initially stored in the refrigerator at 5 °C for 48 h and then stored at 45 °C for another 48 h. After the completion of three cycles of each phase, the formulations were analyzed for any physical instability (i.e. particle dispersion upon manual shaking for 30 s).

Preparation of conventional liposome formulations

Drug-loaded CL-Fs were prepared by using the same method mentioned above with the addition of AmB (the model drug) at a final concentration of 500 µg/mL of the formulation (Table 1). The AmB solution was prepared by dissolving it in a 1:1 v/v cosolvent of chloroform and methanol at a concentration of 150 µg/mL, and the stirring was conducted for 12 h at 1000 rpm in an amber glass bottle at 40 °C.

Formulation optimization

After optimization of BL-Fs, nine AmB-loaded formulations were prepared (Table 1) with varying concentrations of tween61 and SPC, slightly modified based on previously reported methods [13–16]. Moreover, the concentrations of KG, AmB, and PEG400 were kept constant (Table 1).

Preparation of surface-modified liposome formulations

Chondroitin sulfate-coated surface-modified liposome formulations (CS-SML-Fs) were also prepared by the thin film method with a few modifications in the process [11]. Stock solutions of SA, EDC, NHS and CS were prepared initially. In the first step, stearylamine (SA) solution (0.75 M) was prepared by dissolving SA in methanol. In the second step, EDC and NHS were co-dissolved in 1 ml of DDW at a ratio of 2:1 w/w (i.e. 50 and 25 mg/mL) by stirring at 500 rpm for 10 min at RT. In the third step, CS was dissolved as 1 mg/mL in DDW (to the total formulation volume of 10 ml.

For preparation of AmB-loaded CS-SML-Fs, tween61, SPC, KG, AmB and 150 µL of SA solutions were added into a RBF, followed by sonication and evaporation (using similar conditions described earlier). The obtained thin film was then hydrated with 10 ml of aqueous phase containing 26% w/v PEG400 (2.60 g) and kept in a water bath sonicator at 25 °C for 15 min to completely hydrate the thin film. After complete hydration, the formulation was then kept on a magnetic stirrer in an amber glass vial at 900 rpm at RT, and the EDC and NHS solution was added dropwise. This formulation mixture was left for stirring at 900 rpm for up to 1 h for reaction completion. After 1 h, the CS solution was then added gradually. The formulation was kept stirring for another 1 h under similar conditions. After the complete chemical reaction, the formulation was homogenized for 6 min at 20,000 rpm *via* a high-pressure homogenizer at RT. The resultant nanoparticles were then collected by ultracentrifugation using the Optima XPN-80 Ultracentrifuge (Beckman Coulter Ltd, UK) at 20,000 rpm (41200 rcf) at 25 °C for 5 min and washed three times with DDW. The CS-coated AmB-loaded nanoparticle pellets were then collected and re-dispersed in 5 ml of DDW, followed by probe sonication (Q125 sonicator, QSONICA, USA) at 40% amplitude for 10 min at RT. The resultant formulations were then characterized for ZP analysis as well as by Fourier transform infrared (FT-IR) spectroscopy for confirmation of surface-modification and stored in amber glass bottles at three controlled temperatures for stability studies.

Preparation of dye-loaded conventional and surface-modified liposomes

Nile red (NR)-loaded CL-Fs and CS-SML-Fs were prepared using the thin film hydration method (mentioned above Sections). Initially, the lipid phase containing all the components was prepared through rotary evaporation. Then the films were hydrated with the aqueous phase containing 2-5% of the total weight of the final formulations with NR in addition to 26% w/v PEG400 under constant stirring in a water bath and proceeded with the other steps explained before.

Colloidal stability study using physicochemical properties of liposome formulations

Both AmB-loaded CL-Fs and CS-SML-Fs were characterized for PS with PDI, ZP and EE over a period of three months. The samples were stored at three controlled temperatures (5, 25 and 45 °C) in amber glass bottles. The samples were characterized on days-0, 3, 30, and 60. A 10 µL formulation was diluted with 5 ml of DDW for sample preparation, and the mean PS, PDI, and ZP were measured by using dynamic light scattering (DLS) (Zetasizer Nano; Malvern Instruments Ltd, UK) at 25 °C.

An established method of HPLC with optimized conditions was used to quantify AmB entrapment [17]. A HPLC (Agilent 1200 HPLC Instrument, UK) with a UV-visible detector and an Eclipse XDB C18 column (250 mm × 4.6 mm) of 5 µm particle size was used. The mobile phase was comprised of acetonitrile, acetic acid, and deionized water in a ratio of 52:4.3:43.7 v/v/v and adjusted at a flow rate of 1 ml/minute after degassing. The samples were injected at a volume of 20 µL, and the peak areas were recorded at a retention time of 5 min at a wavelength of 406 nm at 25 °C. For calibration, a standard solution of 1 mg/mL AmB was prepared in 80:20 v/v DMSO and methanol and serial dilutions were subsequently prepared in the mobile phase. EE was measured through the direct isocratic method. For the unentrapped drug, 0.5 ml of the formulation was poured into a Millipore filter (10 KD; Fischer Scientific, UK) and centrifuged through benchtop centrifugation (Spectrafuge 24D, Labnet International, USA) for 15 min at 10,000 rpm (12298 rcf), from which the clear filtrate (free or unentrapped drug) was collected for analysis. For the total drug, a 1 ml formulation was lysed with 1 ml of Triton X-100 (1% v/v) to release the entrapped drug followed by a five-fold dilution with the mobile phase. The percentage EE was measured by using the following Equation (1):

$$\%EE = \left(\frac{Total\ added\ drug - Unentrapped\ drug}{Total\ added\ drug} \right) x100 \quad (1)$$

Deformability index of liposome formulations

Membrane extrusion technology was used to evaluate the deformability index (DI) or elasticity of CL-Fs formulated without the elasticizer KG, and CL-Fs and CS-SML-Fs with KG. LipoFast-LF50 extruder (Avestin, Inc., UK) assembly with a semi-permeable polycarbonate (PC) membrane with a 25 mm diameter and 200 nm pore size (Whatman® Nuclepore™ Track-Etched Membranes, Merck, UK) was used for the experiment. A predetermined volume (2-3 ml) of sample was gently pushed through the PC membrane under controlled pressure (5-5.5 bars). The DI of samples was evaluated by the following Equation (2) after quantifying the changes in size before and after extrusion through Zetasizer (Malvern Instruments Ltd, UK).

$$DI = \left(\frac{d_{after} - d_{before}}{d_{before}} \right) x100 \quad (2)$$

Where, DI is the Deformability Index, d_{after} is the mean particle size after undergoing a deformation process (e.g. extrusion), and d_{before} is the mean particle size before undergoing the deformation process.

pH measurement of liposomes

Liposome formulations (1 ml) (CL-Fs without KG, and CL-Fs and CS-SML-Fs with KG) were diluted with 10 ml DDW for pH measurement. A pH meter (Fischer Scientific, UK) was calibrated using standard buffer solutions of pH 4.0 (Hcl) and 7.0 (NaOH), with the electrode rinsed with DDW between calibrations. Subsequently, the calibrated pH electrode was immersed into each sample, and pH readings were allowed to stabilize before recording, with measurements repeated in triplicate for each sample to ensure consistency. Data analysis involved calculating the average pH value and assessing variations between samples.

In vitro drug release study

For the *in-vitro* drug release study of AmB-loaded CS-SML-Fs, a dissolution apparatus (Varian Technology Group, USA) with paddles was used. The temperature was set at 37 ± 1 °C for the medium (400 ml PBS, pH 7.4), and paddle rotation speed was kept at 200 rpm. The CS-SML-Fs were placed in the dialysis tube (MWCD; 10KD) as a barrier to mimic the biological membranes. Samples of 1 ml were withdrawn at predetermined intervals of time (0.5, 1, 2, 3, 4 and 12 h) and replaced with fresh medium to maintain sink conditions. After sample collection, the concentration of drug released was measured *via* HPLC.

Uptake of liposomes by macrophages

Cell culture preparation, cell line, and culture conditions

Monocyte macrophage mouse (ATCC-TIB-67, J774A.1) cells were used for cell uptake studies of liposomes into the cells. The J774A.1 cells were maintained in a complete growth medium comprised of RPMI 1640 with 2 mM L-Glutamine, supplemented with 10% FBS, and antibiotics (50 mg/mL gentamicin, 1% penicillin 10,000 units, and streptomycin 10 mg/mL) in a 75 cm^2 cell culture (T75) flask at 37 °C in a 5% CO_2 incubator for 48 h [18]. The J774A.1 cells were passaged every 3-4 days to maintain optimal growth conditions. The cells were detached from the culture flask using a disposable cell scrapper (Fischer Scientific, UK) upon reaching 80-90% confluency. Subsequently, the detached cells were centrifuged at 1000 rcf for 5 min and resuspended in fresh complete growth medium (5 ml). The cell suspension was then seeded into new T75 culture flasks at a density of 1:5 dilution, and a freshly prepared 10 ml medium was added slowly. The cells were incubated at 37 °C in a 5% CO_2 atmosphere until reaching the desired confluency for subsequent experiments. Medium was replenished every 2-3 days with 10 ml fresh medium added to each flask to ensure sufficient nutrient supply. Passaging was continued until reaching passage number 10, ensuring constant cell behavior and optimal experimental conditions [10, 19].

Cell seeding and treatment

Prior to the experiments, 5 x 10^4 cells/well (750 µL) were seeded into 6-well plates and allowed to adhere for 24 h in an incubator at 37 °C in 5% CO_2 to ensure proper attachment. The supernatant was removed, and subsequently, the culture medium was replaced with fresh medium (2 ml) containing optimized NR-loaded CL-F6, CL-F7, CS-SML-F6, and CS-SML-F9, prepared according to the method described above. The treatment concentration of NR-loaded formulations was 125 µg/mL of AmB (2 ml per well, in triplicates) after serial dilution of the stock solution (500 µg/mL AmB in formulation) and incubation for 1 h at 37 °C in 5% CO_2. Three groups of plates were prepared: (1) the negative control plate (untreated), (2) the NR-loaded liposome formulations plate (treated), and (3) the CS treatment followed by the NR-loaded liposome formulations treated plate.

Flow cytometry analysis

Harvesting and preparations. At the end of incubation, the supernatants were removed, and all the plates were washed three times with cold PBS to remove any free residual nanoparticles or extracellular florescence. Fresh media (2 ml) was added to each well after washing, and cells were detached carefully using a scrapper. Samples were collected in 1.5-ml Eppendorf's tubes and centrifuged at 1000 rcf for 2 min at 4 °C to remove the supernatant [20]. Prior to flow cytometry, the cell pellets were resuspended in 50 µL of fresh culture media [21].

Flow cytometer setup and gating strategy. The BD Accuri C6 flow cytometer was configured with a fast flow rate of 66 µL/minute and featured three blue and one red laser. To isolate the cell population while excluding debris and particles (Figure 1(A)), a dot-plot of forward scatter (FSC-A) vs. side scatter (SSC-A) was employed. Singlet cells were further refined through a dot-plot of FSC-A vs FSC-H (Figure 1(B)). Acquisition limits were determined based on the gating, allowing for a maximum of 5000 events within the singlet gate and utilizing a 50 µL sample volume as a secondary limit. Mean fluorescence intensity (MFI) measurements were collected in FL-3 and FL-4 (M1 and M2 for NR, 550/647 nm on the red channel) (Figure 1(C,D)).

Surface morphology via TEM and SEM

The surface morphology of both CL-Fs and CS-SML-Fs was examined using SEM and TEM to provide insights into their structural characteristics. For SEM, undiluted liposome samples were affixed onto the SEM aluminum stubs over silicon wafer chips of 5x5x0.5 mm dimensions (Agar Scientific Ltd, UK) and air-dried. For TEM, 300 mesh copper grids (Agar Scientific Ltd, UK) were used. An equal volume (50 µL) of liposome sample and ammonium molybdenum (dye) were used during sample preparation and staining for TEM. The diluted sample was applied to the copper grid and air-dried. Upon observation (using both instruments), various images were captured at various magnifications.

Statistical analysis

Statistical analysis involved descriptive assessments performed in Microsoft Excel (2019), calculating mean values and standard deviations for various parameters. Inferential comparisons between nanoformulations employed paired or unpaired t-tests or one-way analysis of variance (ANOVA), generating p-values to determine significance at $p < 0.05$. Each experiment was conducted in triplicate.

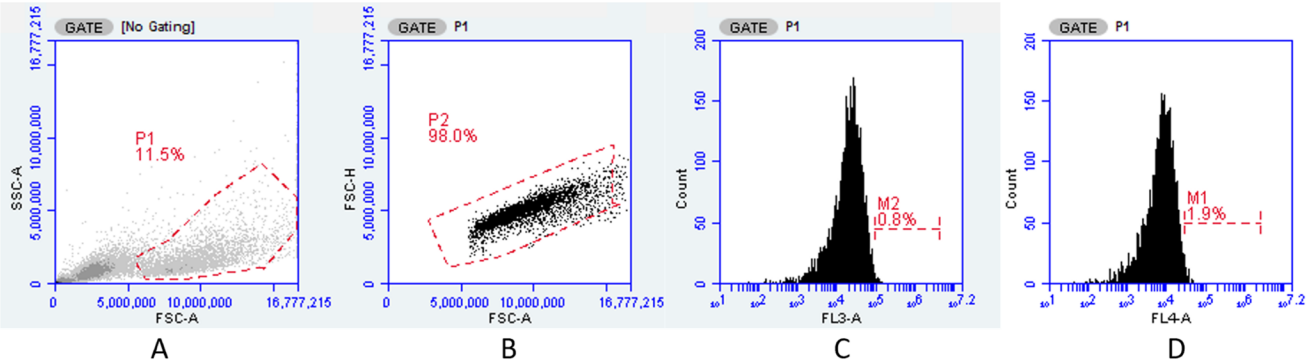

Figure 1. (A) Flow cytometry gating strategy around the cells/P1 gate: FCS-A vs SSC-A (B) Flow cytometry gating strategy around single cells/P2 gate: FCS-A vs FSC-H (C) and (D) FL3-a and FL4-A histograms show gating around negative (M2) and positive (M1) populations.

Results

Thermodynamic stability study of blank liposome formulations

Ten BL-Fs (BL-F1 to BL-F10) were initially prepared after selection of the nonionic surfactant tween61 (HLB value 14) with excellent solubilizing ability for AmB (hydrophobic nature), the lipid SPC due to its higher capacity to encapsulate macromolecules like AmB in order to form stable nanoparticles, and the elasticity inducer KG for its compatibility with topical formulations and clinical effectiveness. All BL-Fs were subjected to a series of thermodynamic stability tests, including overnight stability (at RT), centrifugation, and heating-cooling cycles. The formulations were observed for any kind of phase separation, creaming or precipitation after these steps. All BL-Fs except BL-F5 showed robust physical stability and promptly re-dispersed uniformly after gentle agitation (Table 2). BL-F5 appeared to be very thick, or the formation of large oil droplets appeared due to excess or unbalanced ratios of the surfactant and lipid. These findings underscore the resilience and suitability of the selected nine BL-Fs (Table 2) for further investigation and potential application.

Long-term stability study of conventional and surface-modified liposome formulations

Nine AmB-loaded CL-Fs and CS-SML-Fs were prepared based on the identified stable BL-Fs. These CL-Fs and CS-SML-Fs underwent extensive long-term physical stability to assess any signs of phase separation, drug precipitation, or creaming.

Remarkably, the physical observations revealed a good stability profile for both conventional and surface-modified liposomes stored at 5 °C throughout the entire study period (i.e. 60 days). However, the formulations stored at 25 and 40 °C showed concerning trends. After 30 days, these formulations showed the formation of oil droplets as well as phase separation, which indicated compromised stability at elevated temperatures. These findings emphasize the critical importance of appropriate storage conditions in order to maintain the long-term physical stability of formulations, especially when exposed to higher temperatures.

Colloidal stability study of conventional and surface-modified liposome formulations

Particle size, polydispersity index, and surface charge

On day-0, freshly prepared AmB-loaded CL-Fs exhibited a mean PS ranging from 168-402 nm with a narrow PDI of 0.26-0.44 (Table 3A). Over 60 days, PS was significantly increased ($p < 0.05$), especially at higher temperatures (25 and 40 °C), but remained more stable when stored at 5 °C. The surface charge was negative over all CL-Fs, and at day-0 the ZP ranged from −18.8 to −26.3 mV. Some formulations, including CL-F6, CL-F9, and CL-F10 showed higher stability at 5 °C (showing higher surface charges), while others, including CL-F1, CL-F2 and CL-F3 showed reduced stability at 40 °C on day-30 (Table 3B).

AmB-loaded CS-SML-Fs showed a mean PS ranging from 152.2-190.8 nm, with the exception of CS-SML-F4 (which demonstrated a higher PS of 840.2 nm on day-0), with a PDI ranging from 0.19-0.35 (Table 3A). The PS profile revealed a gradual increase in size for CS-SML-F1, CS-SML-F3, and CS-SML-F4 from day-3 onwards under various storage temperatures. During the long-term stability characterization, CS-SML-F6, CS-SML-F7, CS-SML-F9, and CS-SML-F10 demonstrated a minimal increase in PS at 5 °C. A remarkable stability was shown by CS-SML-F9 (PDI: 0.25-0.32) from day-0 to day-60 at 5 °C. The surface charge over CS-SML-Fs surfaces was also negative before and after linking CS *via* EDC/NHS linkage. The ZP after CS-coating ranged from −28.62 to −40.65 mV, except for CS-SML-F10 (with a shift from a negative to a positive charge), which indicated a loss of CS molecules linked to the surface and showed a positive charge induced by EDC/NHS. The highest ZP (-40.62 to −35 mV) was shown by CS-SML-F9 from day-0 until day-60 at 5 °C, indicated the most stable formulation during long-term storage (Table 3B). These findings suggested the importance of storage conditions in maintaining the stability of the liposome formulations.

Table 2. The overnight stability of blank liposome formulations (BL-Fs) at room temperature. Data are mean ± SD, $n = 3$.

	Overnight stability (at room temperature)	
Formulations	Phase separation/creaming	Stable
BL-F1	No	Yes
BL-F2	No	Yes
BL-F3	No	Yes
BL-F4	No	Yes
BL-F5	Yes	No
BL-F6	No	Yes
BL-F7	No	Yes
BL-F8	No	Yes
BL-F9	No	Yes
BL-F10	No	Yes

Encapsulation efficiency of AmB

The optimized AmB-loaded CL-Fs and CS-SML-Fs demonstrated exceptionally high drug EE of >90%, underscoring their capacity to retain AmB effectively. These AmB-loaded formulations showed EE values greater than 96% (for CL-Fs) and 90% (for CS-SML-Fs) on day-0 (Table 3A). Similar results of higher EE were found after day-60 (Table 3B). Remarkably, EE remained stable at 5 and 25 °C, highlighting the robustness of these formulations. However, a distinct decrease in EE was observed in liposomes subjected to storage at 40 °C, emphasizing the critical role of temperature in maintaining optimal drug encapsulation levels.

Deformability index study

The DI of all CL-Fs prepared with and without elasticity inducer KG (0.1% w/v) and CS-SML-Fs was calculated using the optimized extrusion method [22,23]. The calculated DI values revealed distinct variations across different formulations. For CL-Fs without KG, the highest DI value found was 3.14; whereas for CL-Fs and CS-SML-Fs with KG, the highest DI values were 4.34 and 4.35, respectively. However, some CL-Fs and CS-SML-Fs with KG demonstrated a significant difference ($p < 0.05$) in DI when compared to CL-Fs without KG (Figure 2). These significantly diverse DI values indicate varying degrees of liposome deformability after the addition of the elasticity inducer KG. The CL-Fs with KG (CL-F7 and CL-F10) and CS-SML-Fs (CS-SML-F7 and CS-SML-F9) demonstrated the highest DI values (Figure 2). These findings identified formulations with enhanced deformability, suggesting their potential as effective carriers for enhanced penetration through skin barriers.

pH of liposome formulations

For BL-Fs the pH values remained approximately the same with and without the addition of the deformability inducer KG. Their pH ranged from 5.8-6.0 and 5.7-6.0, showing a minimal effect of KG

Table 3A. Stability studies including particle size, polydispersity index (PDI), zeta potential and entrapment efficiency of AmB-loaded conventional liposome formulations (CL-Fs) and chondroitin sulfate-coated surface-modified liposome formulations (CS-SML-Fs) at day-0 (room temperature) and day-3 under different storage temperatures (5, 25 and 40 °C). Data are mean ± SD, $n = 3$.

	Particle size (nm) and PDI				Zeta potential (mV)				Entrapment efficiency (%)			
	Room temp	5 °C	25 °C	40 °C	Room temp	5 °C	25 °C	40 °C	Room temp	5 °C	25 °C	40 °C
Formulations	Day 0		Day 3		Day 0		Day 3		Day 0		Day 3	
Conventional Liposomes												
CLF-1	275 ± 16.81 (0.36 ± 0.04)	229 ± 7.80 (0.27 ± 0.02)	265 ± 8.22 (0.36 ± 0.06)	275 ± 8.05 (0.5 ± 0.05)	−25.2 ± 3.80	−21.9 ± 1.62	−21.6 ± 1.31	−23.8 ± 0.32	96.2 ± 1.93	99.6 ± 0.33	99.5 ± 0.23	99.7 ± 0.05
CL-F2	307 ± 15.30 (0.31 ± 0.05)	219 ± 1.92 (0.30 ± 0.02)	320 ± 35.32 (0.33 ± 0.02)	320 ± 35.23 (0.6 ± 0.08)	−24.7 ± 2.52	−23.8 ± 0.33	−27.2 ± 4.12	−22.4 ± 1.85	99.5 ± 0.04	99.5 ± 0.35	98.7 ± 0.70	99.1 ± 1.12
CL-F3	217 ± 10.82 (0.41 ± 0.07)	268 ± 9.14 (0.52 ± 0.07)	253 ± 6.90 (0.53 ± 0.08)	337 ± 9.53 (0.7 ± 0.08)	−26.3 ± 3.62	−25.7 ± 0.91	−24.3 ± 1.63	−20.3 ± 1.33	99.6 ± 0.02	99.7 ± 0.06	99.6 ± 0.26	99.5 ± 0.34
CL-F4	267 ± 26.26 0.35 ± 0.05	231 ± 16.05 (0.28 ± 0.03)	236 ± 10.23 (0.27 ± 0.01)	245 ± 2.43 (0.3 ± 0.01)	−19.8 ± 0.53	−21.8 ± 0.51	−20.4 ± 0.83	−20.6 ± 0.34	99.7 ± 0.02	99.6 ± 0.46	94.7 ± 1.54	99.8 ± 0.04
CL-F6	168 ± 11.92 (0.26 ± 0.06)	202 ± 3.84 (0.3 ± 0.07)	211 ± 1.13 (0.36 ± 0.02)	239 ± 2.23 (0.5 ± 0.02)	−23.4 ± 1.85	−25.3 ± 0.93	−23 ± 0.84	−21.1 ± 1.61	99.5 ± 0.06	99.8 ± 0.06	99.6 ± 0.07	99.6 ± 0.08
CL-F7	247 ± 7.54 (0.27 ± 0.02)	344 ± 39.01 (0.43 ± 0.03)	268 ± 12.11 (0.39 ± 0.05)	335 ± 25.03 (0.5 ± 0.1)	−22.5 ± 3.23	−21.7 ± 0.71	−20.9 ± 0.80	−21.1 ± 1.62	99.7 ± 0.04	99.8 ± 0.01	99.5 ± 0.34	99.5 ± 0.31
CL-F8	402 ± 17.02 (0.44 ± 0.04)	328 ± 15.21 (0.31 ± 0.09)	330 ± 5.23 (0.34 ± 0.02)	348 ± 12.32 (0.4 ± 0.1)	−21.6 ± 1.24	−23.1 ± 0.93	−22.8 ± 0.33	−23.8 ± 0.42	99.5 ± 0.32	99.3 ± 0.36	94.5 ± 1.74	99.3 ± 0.02
CL-F9	234 ± 5.24 (0.27 ± 0.06)	238 ± 5.91 (0.28 ± 0.01)	252 ± 4.95 (0.32 ± 0.03)	298 ± 4.34 (0.4 ± 0.04)	−24.0 ± 2.22	−25.8 ± 2.81	−22.6 ± 4.26	−21.8 ± 2.24	97 ± 1.02	99.7 ± 0.11	99.5 ± 0.35	99.8 ± 0.12
CL-F10	248 ± 20.01 (0.26 ± 0.05)	232 ± 2.53 (0.28 ± 0.02)	221 ± 13.72 (0.24 ± 0.02)	247 ± 2.53 (0.3 ± 0.04)	−18.8 ± 0.44	−25.2 ± 0.55	−23.5 ± 0.08	−24 ± 0.23	99.4 ± 0.12	99.3 ± 0.32	99.6 ± 0.02	99.1 ± 0.11
Surface-modified Liposomes												
CS-SML-F1	188 ± 5.71 (0.2 ± 0.01)	331 ± 47.23 (0.3 ± 0.01)	651 ± 59.02 (0.2 ± 0.004)	2415 ± 163.3(0.5 ± 0.02)	−35.5 ± 0.72	−36 ± 0.71	−31 ± 0.98	−46 ± 10.43	90.6 ± 0.95	99.6 ± 0.11	99.5 ± 0.45	99.2 ± 0.81
CS-SML-F3	176 ± 6.40 (0.3 ± 0.007)	336 ± 17.72 (0.2 ± 0.04)	364 ± 14.30 (0.4 ± 0.003)	1094 ± 10.02 (0.6 ± 0.01)	−29.8 ± 5.73	−31.4 ± 3.31	−34 ± 0.95	−36 ± 0.50	99.6 ± 0.21	90.8 ± 0.55	99.8 ± 0.14	99.6 ± 0.04
CS-SML-F4	840 ± 17.20 (0.4 ± 0.02)	629 ± 5.33 (0.4 ± 0.04)	1146 ± 12.14 (0.3 ± 0.02)	637 ± 222.31 (0.5 ± 0.05)	−29.5 ± 0.45	−26 ± 0.05	−26 ± 0.05	−33 ± 0.25	99.6 ± 0.11	99.2 ± 0.72	99.9 ± 0.03	99.7 ± 0.04
CS-SML-F6	152 ± 1.93 (0.3 ± 0.01)	227 ± 4.90 (0.3 ± 0.01)	242 ± 3.35 (0.3 ± 0.001)	335 ± 4.60 (0.6 ± 0.002)	−33 ± 0.05	−33 ± 0.25	−33 ± 0.22	−34 ± 0.41	99.5 ± 0.40	99.7 ± 0.23	99.8 ± 0.05	97.5 ± 0.30
CS-SML-F7	164 ± 1.19 (0.2 ± 0.01)	220 ± 1.23 (0.3 ± 0.002)	505 ± 8.91 (0.9 ± 0.04)	263 ± 73.23 (0.4 ± 0.04)	−37 ± 0.95	−37 ± 0.52	−34 ± 0.45	−32 ± 0.44	99.6 ± 0.12	99.9 ± 0.15	99.9 ± 0.11	87.8 ± 0.93
CS-SML-F9	191 ± 0.63 (0.3 ± 0.0005)	183 ± 3.20 (0.2 ± 0.01)	186 ± 1.25 (0.2 ± 0.001)	189 ± 2.12 (0.3 ± 0.02)	−41 ± 1.34	−41 ± 1.51	−41 ± 0.32	−41 ± 0.45	98.9 ± 0.51	99.8 ± 0.23	99.9 ± 0.17	99.7 ± 0.22
CS-SML-F10	177 ± 1.92 (0.3 ± 0.01)	243 ± 11.50 (0.4 ± 0.001)	258 ± 6.05 (0.3 ± 0.002)	293 ± 2.23 (0.4 ± 0.01)	−28.7 ± 0.35	28.7 ± 0.65	−28 ± 0.11	29 ± 0.41	99.1 ± 0.04	98.6 ± 0.21	98 ± 0.11	98.2 ± 0.82

Table 3B. Stability studies including particle size, polydispersity index (PDI), zeta potential and entrapment efficiency of AmB-loaded conventional liposome formulations (CL-Fs) and chondroitin sulfate-coated surface-modified liposome formulations (CS-SML-Fs) at day 30 and day 60 under different storage temperatures (5, 25 and 40 °C). Data are mean ± SD, $n = 3$.

	Particle size (nm) and PDI			Zeta potential (mV)			Entrapment efficiency (%)		
Formulations	5 °C	25 °C	40 °C	5 °C	25 °C	40 °C	5 °C	25 °C	40 °C
Conventional liposome									
Day 30									
CLF-1	226 ± 5.92 (0.32 ± 0.06)	381 ± 30.02 (0.47 ± 0.12)	1026 ± 41.56 (0.74 ± 0.05)	−28.7 ± 0.82	−27.2 ± 0.85	−13.7 ± 0.61	99.7 ± 0.03	99.5 ± 0.22	91.4 ± 1.73
CL-F2	315 ± 9.62 (0.54 ± 0.07)	364 ± 13.42 (0.46 ± 0.02)	627 ± 52.43 (0.85 ± 0.07)	−26.8 ± 0.41	−28.8 ± 1.33	−15.6 ± 1.30	99.7 ± 0.12	99.6 ± 0.20	85.6 ± 0.52
CL-F3	295 ± 7.74 (0.44 ± 0.07)	481 ± 229.32 (0.65 ± 0.30)	2314 ± 246.23 (0.86 ± 0.24)	−16.8 ± 5.12	−29.3 ± 4.50	−12.8 ± 2.42	99.9 ± 0.03	99.3 ± 0.14	93.2 ± 1.21
CL-F4	251 ± 8.02 (0.40 ± 0.03)	272 ± 14.50 (0.5 ± 0.07)	1219 ± 23.36 (0.93 ± 0.05)	−21.5 ± 2.91	−23.2 ± 2.93	−20.2 ± 1.22	98.1 ± 0.23	99.5 ± 0.16	93.3 ± 0.54
CL-F6	424 ± 242.20 (0.42 ± 0.15)	604 ± 225.31 (0.33 ± 0.06)	1688 ± 912.11 (1 ± 0.01)	−26.2 ± 0.52	−24.6 ± 2.41	−19.2 ± 1.73	99.3 ± 0.35	91.1 ± 0.56	95.3 ± 0.50
CL-F7	335 ± 25.32 (0.45 ± 0.05)	815 ± 555.35 (0.38 ± 0.26)	1816 ± 191.14 (0.93 ± 0.03)	−25.4 ± 2.93	−26.4 ± 3.82	−21.2 ± 1.52	99.2 ± 0.83	99.3 ± 0.03	93.9 ± 0.52
CL-F8	348 ± 12.05 (0.30 ± 0.01)	379 ± 6.26 (0.3 ± 0.11)	2017 ± 58.31 (0.84 ± 0.08)	−22.4 ± 2.41	−26.8 ± 4.82	−22.2 ± 0.93	99.5 ± 0.22	99.7 ± 0.03	92.3 ± 2.35
CL-F9	262 ± 2.55 (0.3 ± 0.03)	367 ± 181.20 (0.3 ± 0.21)	1991 ± 43.14 (0.6 ± 0.05)	−25.3 ± 0.22	−37.2 ± 0.93	−21.1 ± 0.65	99.9 ± 0.52	95.9 ± 0.13	93 ± 0.94
CL-F10	224 ± 5.63 (0.3 ± 0.03)	358 ± 177.23 (0.4 ± 0.06)	1108 ± 242.02 (0.71 ± 0.03)	−21.5 ± 1.85	−29.5 ± 5.41	−22.1 ± 2.30	99.4 ± 0.02	99.4 ± 0.14	96.2 ± 0.34
Day 60									
CLF-1	245 ± 10.33 (0.4 ± 0.08)	1508 ± 1460.21 (0.42 ± 0.2)	3986 ± 656.15 (0.9 ± 0.11)	−28.9 ± 0.53	−24.4 ± 4.71	−23.1 ± 2.74	99.6 ± 0.02	92.1 ± 0.31	92 ± 0.83
CL-F2	259 ± 9.45 (0.4 ± 0.02)	1483 ± 140.23 (0.6 ± 0.04)	2241 ± 179.10 (0.7 ± 0.04)	−29.4 ± 0.21	−30.3 ± 16.50	−22.2 ± 1.52	99.7 ± 0.11	95.9 ± 0.45	93 ± 0.16
CL-F3	271 ± 4.83 (0.4 ± 0.02)	1119 ± 335.21 (0.5 ± 0.33)	1846 ± 169.22 (0.7 ± 0.23)	−28.9 ± 0.51	−36.2 ± 12.40	−20.4 ± 7.83	97.1 ± 0.21	96.9 ± 0.26	92.5 ± 1.01
CL-F4	364 ± 16.02 (0.5 ± 0.11)	1163 ± 1222.31 (0.5 ± 0.06)	1043 ± 132.40 (0.9 ± 0.09)	−25.3 ± 5.72	−28.5 ± 2.26	−21.6 ± 2.14	99.6 ± 0.01	93.5 ± 1.05	91 ± 0.81
CL-F6	408 ± 292.31 (0.3 ± 0.11)	3343 ± 1823.25 (0.8 ± 0.32)	1288 ± 879.34 (0.8 ± 0.15)	−34.1 ± 1.61	−31.2 ± 1.15	−18.1 ± 2.03	95.3 ± 0.43	93.2 ± 0.12	86.2 ± 0.83
CL-F7	273 ± 33.24 (0.3 ± 0.08)	2665 ± 349.25 (0.6 ± 0.41)	5815 ± 130.05 (1.0 ± 0.01)	−29.4 ± 6.30	−31.1 ± 9.53	−36.1 ± 8.33	99.2 ± 0.42	92.4 ± 2.42	89.2 ± 0.84
CL-F8	338 ± 9.43 (0.4 ± 0.01)	2076 ± 257.23 (0.3 ± 0.05)	1359 ± 354.25 (0.9 ± 0.05)	−28.7 ± 8.41	−23.2 ± 4.62	−17.1 ± 4.43	99.8 ± 0.12	93.4 ± 1.01	36.5 ± 5.94
CL-F9	284 ± 18.24 (0.3 ± 0.04)	973 ± 478.35 (0.7 ± 0.25)	1729 ± 502.45 (0.8 ± 0.22)	−34.2 ± 4.13	−40.3 ± 7.94	−26.2 ± 6.52	96.5 ± 0.35	99.3 ± 0.53	84.2 ± 2.08
CL-F10	241 ± 14.20 (0.3 ± 0.07)	2572 ± 1299.20 (0.7 ± 0.22)	1947 ± 243.45 (0.9 ± 0.13)	−33.2 ± 5.11	−26.5 ± 3.83	19.6 ± 6.54	94.8 ± 0.92	98.4 ± 0.64	45.6 ± 4.32
Surface modified liposome									
Day 30									
CS-SML-F1	1584 ± 114.09 (0.3 ± 0.01)	2241 ± 74.23 (0.8 ± 0.01)	3339 ± 8.52 (0.7 ± 0.01)	−26.3 ± 0.90	−19.6 ± 0.70	−19.2 ± 1.72	99.7 ± 0.33	99.6 ± 0.31	64.4 ± 1.14
CS-SML-F3	948 ± 289.23 (0.2 ± 0.05)	1134 ± 78.54 (0.6 ± 0.02)	5080 ± 42.51 (0.3 ± 0.01)	−25.3 ± 1.10	−30.4 ± 0.01	−26.2 ± 0.61	99.7 ± 0.31	99.2 ± 0.03	99.1 ± 0.73
CS-SML-F4	3125 ± 536.41 (0.4 ± 0.04)	2053 ± 55.52 (0.3 ± 0.01)	4119 ± 55.32 (0.7 ± 0.05)	−28.3 ± 1.02	−19.3 ± 0.50	−18.4 ± 0.22	99.6 ± 0.15	99.8 ± 0.22	99.3 ± 0.71
CS-SML-F6	334 ± 5.73 (0.3 ± 0.001)	383 ± 14.51 (0.5 ± 0.01)	1072 ± 50.53 (0.8 ± 0.02)	−25.5 ± 0.20	−40.1 ± 0.30	−31.9 ± 0.16	99.7 ± 0.01	99.6 ± 0.04	74.2 ± 2.02
CS-SML-F7	239 ± 3.74 (0.6 ± 0.02)	512 ± 12.53 (0.9 ± 0.01)	2362 ± 47.25 (0.8 ± 0.02)	−37.2 ± 0.05	−34.2 ± 0.70	−30.8 ± 0.34	99.8 ± 0.03	99.3 ± 0.23	98.4 ± 1.04
CS-SML-F9	191 ± 1.63 (0.3 ± 0.02)	200 ± 0.82 (0.3 ± 0.01)	4476 ± 146.43 (0.7 ± 0.03)	−41.2 ± 1.10	−41.3 ± 0.20	−41.2 ± 0.23	99.7 ± 0.23	99.5 ± 0.03	99.3 ± 0.82
CS-SML-F10	213 ± 2.25 (0.6 ± 0.04)	222 ± 1.55 (0.7 ± 0.02)	5244 ± 120.22 (0.9 ± 0.04)	28.2 ± 0.30	28.2 ± 0.05	20.2 ± 0.31	98.3 ± 0.72	98.2 ± 0.11	98.1 ± 0.73
Day 60									
CS-SML-F1	2308 ± 103.34 (0.2 ± 0.004)	1089 ± 24.62 (0.3 ± 0.03)	4835 ± 20.02 (0.9 ± 0.02)	−14.6 ± 0.21	−21.4 ± 0.73	−31.4 ± 1.82	98.5 ± 0.05	99.5 ± 0.52	61.5 ± 1.82
CS-SML-F3	1231 ± 46.21 (0.1 ± 0.004)	1495 ± 11.32 (0.6 ± 0.02)	2074 ± 53.71 (0.9 ± 0.01)	−17.8 ± 0.63	−22.3 ± 0.21	−32.2 ± 0.51	97.8 ± 0.08	99.8 ± 0.13	64.3 ± 0.61
CS-SML-F4	1603 ± 70.54 (0.5 ± 0.04)	1235 ± 6.54 (0.6 ± 0.02)	1690 ± 13.41 (0.8 ± 0.01)	−24.3 ± 0.24	−12.4 ± 1.15	−30.5 ± 0.55	98.6 ± 0.11	99.2 ± 0.11	64.2 ± 0.63
CS-SML-F6	383 ± 3.21 (0.3 ± 0.002)	1477 ± 33.23 (0.4 ± 0.03)	3646 ± 25.53 (0.9 ± 0.01)	−27.2 ± 0.21	−24.5 ± 0.52	−26.3 ± 0.32	87.3 ± 0.72	89.3 ± 0.92	89.4 ± 0.61
CS-SML-F7	231 ± 2.22 (0.3 ± 0.01)	3259 ± 11.53 (0.3 ± 0.001)	5328 ± 34.35 (0.9 ± 0.01)	−33.4 ± 0.51	−25.5 ± 0.82	−35 ± 0.15	95.7 ± 0.33	99.4 ± 0.54	85.3 ± 0.64
CS-SML-F9	281 ± 1.45 (0.3 ± 0.003)	1477 ± 83.24 (0.4 ± 0.01)	1457 ± 42.23 (0.7 ± 0.01)	−35.2 ± 1.32	−17.4 ± 2.13	−24 ± 1.75	99.5 ± 0.42	97.4 ± 0.31	85.7 ± 0.02
CS-SML-F10	198 ± 1.85 (0.2 ± 0.002)	616 ± 11.32 (0.2 ± 0.02)	1005 ± 46.25 (0.5 ± 0.01)	26.1 ± 0.22	−21.2 ± 0.33	−26 ± 0.13	99.7 ± 0.44	99.2 ± 0.04	91.3 ± 0.53

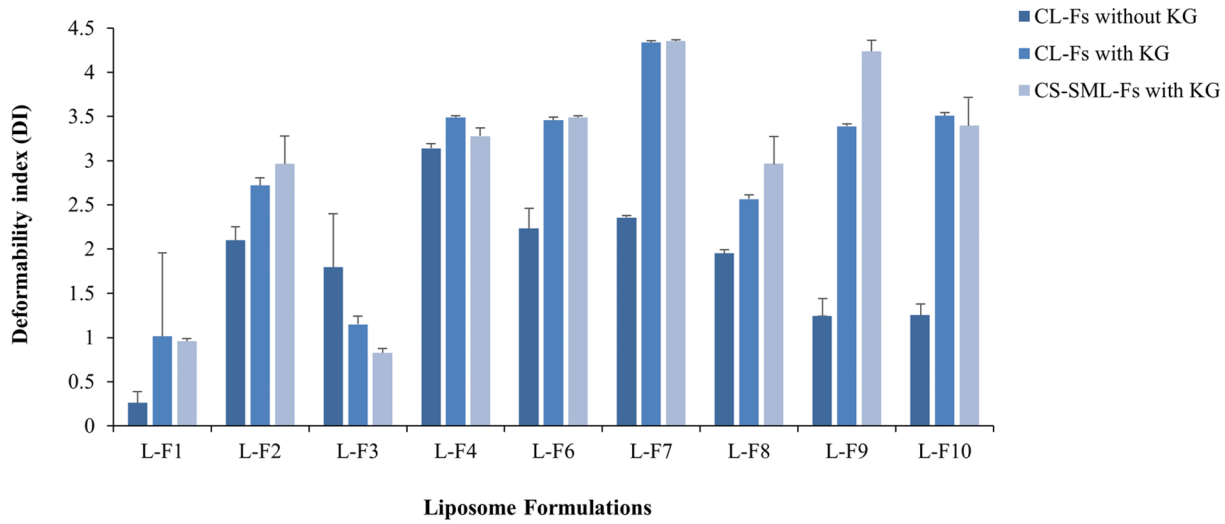

Figure 2. Deformability index of conventional liposome formulations (CL-Fs) without and with dipotassium glycyrrhizinate (KG), and chondroitin sulfate-coated surface-modified formulations (CS-SML-Fs) with KG. Data are mean ± SD, $n = 3$.

Table 4. pH Of blank liposome formulations (BL-Fs) without and with dipotassium glycyrrhizinate (KG), AmB-loaded conventional liposome formulations (CL-Fs), and chondroitin sulfate-coated surface-modified liposome formulations (CS-SML-Fs). Data are mean ± SD, $n = 3$.

	BL-Fs			
Formulations	without KG	with KG	CL-Fs	CS-SML-Fs
F1	5.8 ± 0.03	5.8 ± 0.03	5.8 ± 0.02	6.8 ± 0.02
F2	5.7 ± 0.02	5.7 ± 0.02	5.7 ± 0.15	5.7 ± 0.03
F3	6.2 ± 0.03	5.9 ± 0.03	5.6 ± 0.04	5.5 ± 0.02
F4	6.2 ± 0.14	6.3 ± 0.14	5.7 ± 0.05	7.3 ± 0.11
F6	6.0 ± 0.01	6.0 ± 0.01	5.7 ± 0.03	7.2 ± 0.07
F7	6.0 ± 0.07	6.0 ± 0.07	5.8 ± 0.01	7.0 ± 0.07
F8	5.9 ± 0.06	5.9 ± 0.06	5.8 ± 0.05	7.0 ± 0.01
F9	5.9 ± 0.03	5.9 ± 0.03	5.7 ± 0.04	7.4 ± 0.07
F10	5.9 ± 0.03	5.8 ± 0.03	5.7 ± 0.05	7.3 ± 0.09

on liposome nature. Similarly, CL-Fs displayed pH values ranging from 5.6-6.0, whereas CS-SML-Fs showed a slightly broader pH range of 5.5–7.4 (Table 4). These findings are attributed to the relatively stable pH characteristics of the liposomes, which is crucial for their compatibility with the physiological conditions of the skin and potential drug delivery applications.

In vitro drug release study

The drug release profiles of AmB for the six optimized AmB-loaded CS-SML-Fs (CS-SML-F1, CS-SML-F3, CS-SML-F4, CS-SML-F6, CS-SML-F7 and CS-SML-F9) were determined over a time period of 12 h (Figure 3). As depicted, these formulations exhibited sustained release behavior with a gradual increase in concentration after 2 h of duration in the receptor medium. While all formulations exhibited sustained release behavior, the CS-SML-F9 stands out as having the highest concentration of drug release rate over the study duration. The controlled release profile makes the liposome formulations suitable for low dosing frequencies.

Cell uptake analysis of liposomes by flow cytometry

In the cell uptake study, macrophage J774A.1 cells were employed, and the estimated quantitative uptake of AmB from different formulations demonstrated higher values for the CS-SML-F9 formulation. The cells showed a significantly higher MFI in the FL-3 channel compared to the other formulations (CL-F6, CL-F9) and the negative control (Figure 4). Interestingly, CS-SML-F6 showed a significantly lower ($p < 0.05$) cellular uptake when compared to CS-SML-F9. The CS-pretreatment group, followed by NR-loaded liposome treatment, displayed lower uptake profiles compared to the other two groups (Figure 4). This reduction in uptake in the CS-pretreatment group is likely attributable to the ability of CS to competitively block receptor sites (cysteine-rich domains) on the surface of macrophages, thereby hindering the uptake of NR-loaded liposomes. These findings showed a pivotal role of surface-modification for targeted drug delivery.

Surface morphology

TEM and SEM were used to study the surface morphology of AmB-loaded CL-F9 and CS-SML-F9. TEM images of AmB-loaded liposomes (Figure 5(A,B)) confirmed the structural integrity of the nanoparticles, which showed a spherical and uniform distribution. The images showed there was no disruption in the structure of the liposomes after extensive mechanical stresses from high-pressure homogenization and probe sonication. Furthermore, SEM images provide detailed information about the CL-F9 and CS-SML-F9 nanoparticles. Clear spherical shapes with uniformity across the particles are evident, indicating consistent PS and shape within the formulations (Figure 5(C,D)). Additionally, the images show minimal particle agglomeration, suggesting good dispersibility and stability of the liposomal nanoparticles.

Discussion

Effective drug delivery systems are required in order to improve the therapeutic efficacy of drugs and minimize their side effects. As previous studies showed, optimized drug delivery can improve bioavailability, control drug release, and enable targeted drug delivery to specific receptors, enhancing therapeutic outcomes and reducing potential adverse effects [24]. The available generic dosage forms of AmB face challenges such as poor water solubility, membrane permeability, infusion-related reactions, systemic

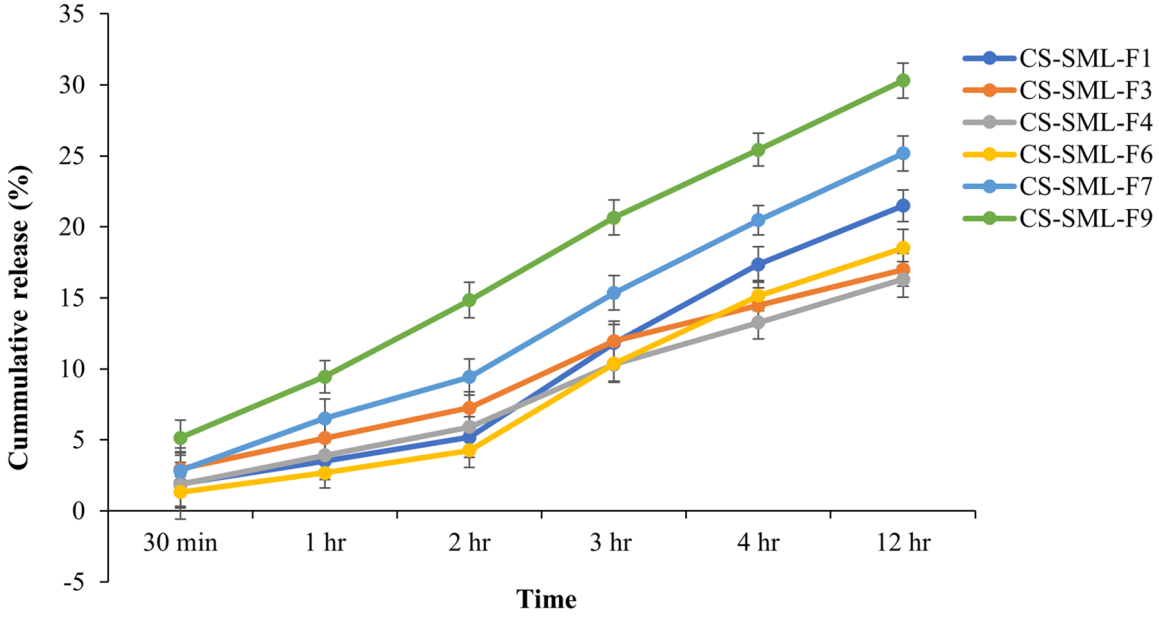

Figure 3. The cumulative percentage *in-vitro* drug release of AmB from the chondroitin sulfate-coated surface-modified liposome formulations (CS-SML-Fs) over a time period of 12 h. Data are mean ± SD, $n = 3$.

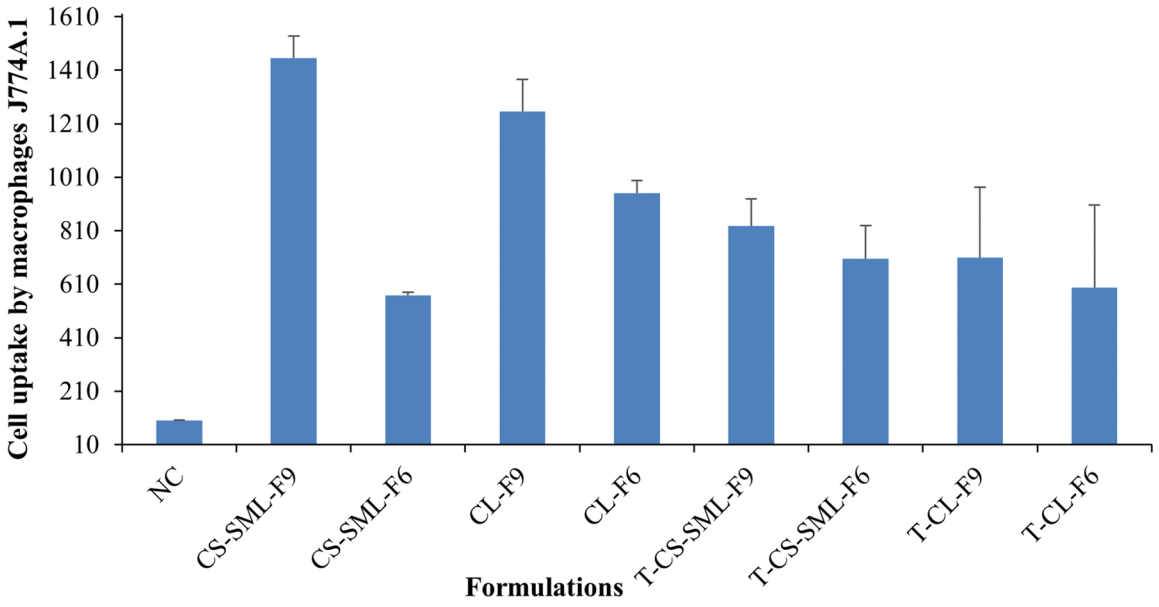

Figure 4. Flow cytometry analysis of liposomal formulation uptake by murine macrophage J774A.1 cells, where negative control (NC), chondroitin sulfate surface-modified liposome formulations (CS-SML-Fs), conventional liposome formulation (CL-Fs), and pretreatment group with chondroitin sulfate (T-CS-SML-Fs and T-CL-Fs). Data are mean ± SD, $n = 3$.

toxicity (including hepatotoxicity and cardiotoxicity), and other side effects. In contrast, lipid-based nanoparticles (for example, liposomes) and other polymeric nano- and microparticles provide advantages including increased bioavailability, drug stability, and targeted delivery. These lipid-based nanoparticles also enhance entrapment efficiency, reduce drug leakage, and provide greater stability upon storage (Table 3) [1]. CS-modified nanoparticles for delivering AmB specifically to macrophages have been explored due to the expression of chondroitin receptors on macrophages [25]. By targeting macrophages, these nanoparticles aim to enhance therapeutic efficacy while reducing first-pass metabolism and the systemic side effects of AmB [18].

Macrophages play a crucial role in targeting and eliminating pathogens, making them a significant target for drug delivery in various diseases. Improving the efficiency of drug uptake by macrophages can enhance therapeutic outcomes, yet traditional drug delivery systems often fall short of delivering drugs effectively to these cells. However, CS is a naturally occurring biopolymer and is of significant importance in drug delivery due to its biodegradability, biocompatibility, cost-effectiveness and anti-inflammatory properties [26,27]. CS can interact with macrophage receptors (Figure 4), such as CD44, facilitating targeted drug delivery [28]. In the process of modifying liposomes with CS, carbodiimide using EDC and NHS is commonly employed to covalently attach it to the

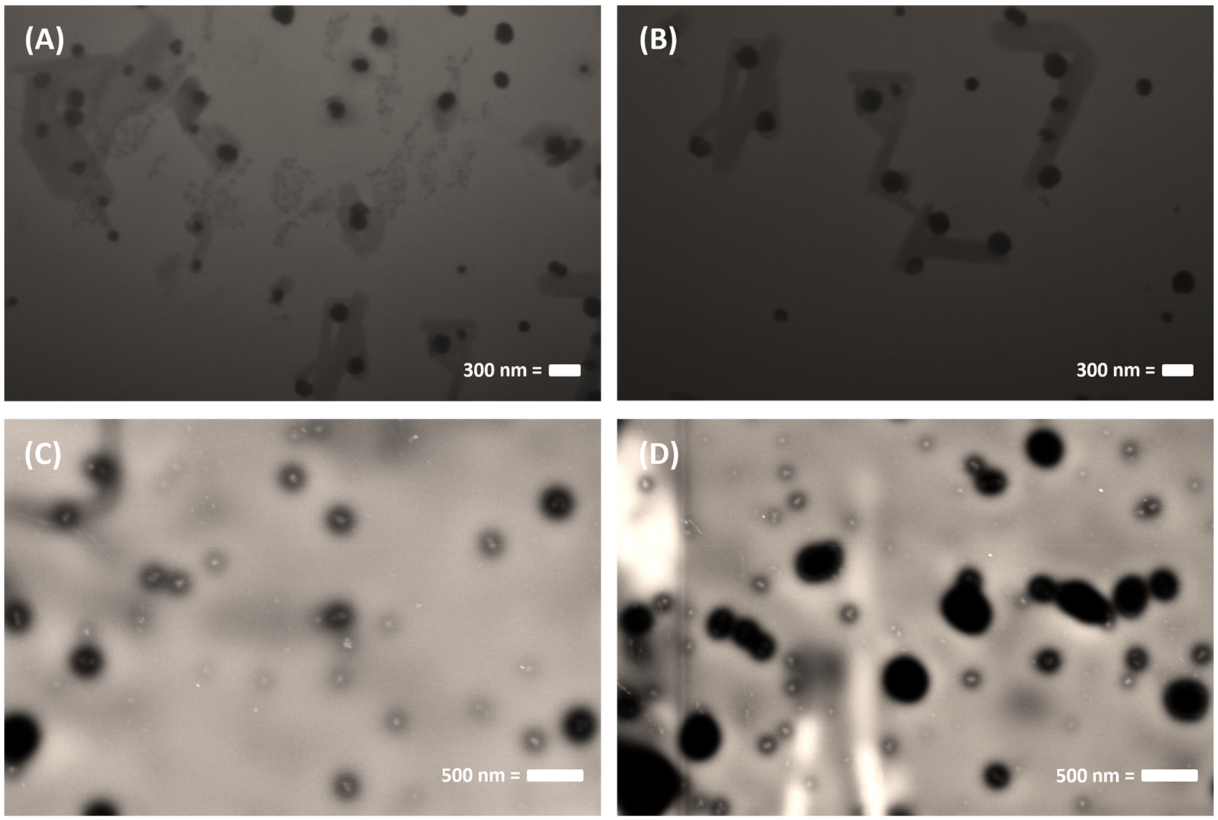

Figure 5. Surface morphology *via* transmission electron microscopy (TEM) images of AmB-loaded (A) conventional (CL-F9) and (B) surface-modified liposome formulation (CS-SML-F9); as well as scanning electron micrographs of AmB-loaded (C) conventional (CL-F9) and (D) surface-modified liposome formulation (CS-SML-F9). These images are typical of three such different experiments.

liposomes. This process involves activating the carboxyl groups of CS and reacting them with the amine groups present on the liposome surface [29]. The functionalized PEG400 serves as a flexible linker arm, extending the CS away from the liposome surface and potentially enhancing bioavailability and targeting capability. By avoiding steric hindrance and improving stability, this approach can lead to more effective and targeted drug delivery to macrophages [12].

The MR expressed on various cell types, including macrophages, dendritic cells, and endothelial cells, plays a pivotal role in immune responses and hormonal clearance. Specifically, the membrane-distal cysteine-rich domain of the MR binds to sulfated carbohydrates, facilitating interactions with various ligands. Recent studies have identified two novel classes of carbohydrate ligands for the cysteine-rich domain: firstly, chondroitin-4 sulfate chains found on proteoglycans produced by immune cells, and secondly, sulfated blood group chains [28]. Furthermore, the occurrence of CS chains in extracellular matrices suggests a role in directing the trafficking of macrophages and other MR-bearing cells to pathological tissues. Several parasites, like leishmanial strains, reside within the phagosomes and hence restrict the activity of several drugs that are otherwise effective against the extracellular species. Drug targeting into macrophages by exploiting the MR-subunits expressed on the cell surface presents a great opportunity for drugs to specifically target the pathogens by delivering the drugs into the macrophages [30]. The cysteine-rich domain helps in the internalization of the CS-modified nanoparticles by utilizing the mechanism described for binding the sulfated carbohydrate chains.

This study explored the uptake and penetration of modified nanoparticles into the murine macrophages carrying AmB by targeting the cysteine-rich domain site of the MR. Liposomes can further enhance drug penetration in the presence of penetration enhancers like KG (Figure 2), which can also provide anti-inflammatory and emollient effects [31]. In the present study, CS-SML-Fs were prepared with reproducible and scalable methods resulting in high EE, with the use of SPC providing greater flexibility to the liposome bilayer. The SPC lipid concentric bilayer also provided stability to retain AmB within the liposome bilayer [1]. While similar to the marketed formulation, AmBisome®, the EE was very high (>95%). The method of preparation showed scalable properties as the formulations showed effective PS, ZP, PDI and EE over a storage period of six months at 5 °C (Table 3). The uptake of CS-SML-Fs by J774A.1 cells might occur by adsorption or incorporation with the MR on the surface of J774A.1 cells. The difference between the uptake of CL-Fs and CS-SML-Fs was estimated by the florescence intensity of NR dye detected by flow cytometry (Figure 4). These results suggested that conventional liposome uptake was low by the cells due to their lower interaction with the cysteine-rich domain of MR. Figure 4 also exhibited the interaction of CS-SML-F6 and CS-SML-F9 with J774A.1 cells with an increased intensity of fluorescence. This method is advantageous in quantifying the interaction of nanoformulations with the cells.

Conclusions

In this study, BL-Fs were designed and optimized to prepare and engineer CL-Fs and CS-SML-Fs for topical drug delivery using AmB as a model drug. It is vital to know that the development of effective drug delivery systems is imperative for enhancing therapeutic

outcomes while minimizing side effects. Liposomes, propose significant advantages over conventional formulations by improving drug bioavailability, stability, and targeted delivery. CS-SML-Fs represented a promising strategy for higher drug uptake by macrophages, which play a critical role in fighting infections. The interaction of CS-modified nanoparticles with macrophage receptors, such as the MR, facilitated targeted drug delivery, potentially improved therapeutic efficacy, and reduced systemic toxicity. This study demonstrated the successful uptake and penetration of CS-modified nanoparticles into murine macrophages carrying AmB, suggesting their potential utility in targeted drug delivery against intracellular pathogens. Further research and clinical trials are warranted to validate their efficacy and safety in clinical settings, ultimately contributing to the development of more effective and safer therapeutic interventions against infectious diseases.

Disclosure statement

No potential conflict of interest was reported by the author(s).

Funding

The author(s) reported there is no funding associated with the work featured in this article.

Data availability statement

The authors declare that all the supporting data are contained within the paper.

References

[1] Jaafari MR, Hatamipour M, Alavizadeh SH, et al. Development of a topical liposomal formulation of amphotericin b for the treatment of cutaneous leishmaniasis. Int J Parasitol Drugs Drug Resist. 2019;11:156–165. doi: 10.1016/j.ijpddr.2019.09.004.

[2] Ribeiro TG, Chávez-Fumagalli MA, Valadares DG, et al. Novel targeting using nanoparticles: an approach to the development of an effective anti-leishmanial drug-delivery system. Int J Nanomedicine. 2014;9:877–890. doi: 10.2147/IJN.S55678.

[3] Bangham AD, Standish MM, Watkins JC. Diffusion of univalent ions across the lamellae of swollen phospholipids. J Mol Biol. 1965;13(1):238–252. 238-IN27. doi: 10.1016/s0022-2836(65)80093-6.

[4] Khan I, Al-Hasani A, Khan MH, et al. Impact of dispersion media and carrier type on spray-dried proliposome powder formulations loaded with beclomethasone dipropionate for their pulmonary drug delivery via a next generation impactor. PLoS One. 2023;18(3):e0281860. doi: 10.1371/journal.pone.0281860.

[5] Hollmerus S, Yousaf S, Islam Y, et al. Isoflavones-based liposome formulations as anti-aging for skincare. NAPDD. 2018;3(3):28–37. doi: 10.19080/NAPDD.2018.03.555615.

[6] Ansam M, Yousaf S, Bnyan R, et al. Anti-aging liposomal formulation. Mini Review. Novel Approaches in Drug Designing and Development. 2018;3:66–68.

[7] Mathew Thevarkattil A, Yousaf S, Houacine C, et al. Anticancer drug delivery: investigating the impacts of viscosity on lipid-based formulations for pulmonary targeting. Int J Pharm. 2024;664:124591. doi: 10.1016/j.ijpharm.2024.124591.

[8] Khan I, Yousaf S, Subramanian S, et al. Proliposome tablets manufactured using a slurry-driven lipid-enriched powders: development, characterization and stability evaluation. Int J Pharm. 2018;538(1-2):250–262. doi: 10.1016/j.ijpharm.2017.12.049.

[9] Abdullah TA, Ibrahim NJ, Warsi MH. Chondroitin sulfate-chitosan nanoparticles for ocular delivery of bromfenac sodium: improved permeation, retention, and penetration. Int J Pharm Investig. 2016;6(2):96–105. doi: 10.4103/2230-973X.177823.

[10] Thoo L, Fahmi MZ, Zulkipli IN, et al. Interaction and cellular uptake of surface-modified carbon dot nanoparticles by j774.1 macrophages. Cent Eur J Immunol. 2017;42(3):324–330. doi: 10.5114/ceji.2017.70978.

[11] Zu M, Ma L, Zhang X, et al. Chondroitin sulfate-functionalized polymeric nanoparticles for colon cancer-targeted chemotherapy. Colloids Surf B Biointerfaces. 2019;177:399–406. doi: 10.1016/j.colsurfb.2019.02.031.

[12] Ficko-Blean E. A fresh trim provides a new look at the human mannose receptor. J Biol Chem. 2021;297(1):100922. doi: 10.1016/j.jbc.2021.100922.

[13] Hussain A, Samad A, Singh S, et al. Nanoemulsion gel-based topical delivery of an antifungal drug: in vitro activity and in vivo evaluation. J. Drug Deliv. 2016;23(2):642–647. doi: 10.3109/10717544.2014.933284.

[14] Hussain A, Samad A, Singh SK, et al. Enhanced stability and permeation potential of nanoemulsion containing sefsol-218 oil for topical delivery of amphotericin b. Drug Dev Ind Pharm. 2015;41(5):780–790. doi: 10.3109/03639045.2014.902957.

[15] Hussain A, Singh VK, Singh OP, et al. Formulation and optimization of nanoemulsion using antifungal lipid and surfactant for accentuated topical delivery of amphotericin b. J. Drug Deliv. 2016;23(8):3101–3110. doi: 10.3109/10717544.2016.1153747.

[16] Manosroi A, Chankhampan C, Manosroi W, et al. Transdermal absorption enhancement of papain loaded in elastic niosomes incorporated in gel for scar treatment. Eur J Pharm Sci. 2013;48(3):474–483. doi: 10.1016/j.ejps.2012.12.010.

[17] Espada R, Josa J, Valdespina S, et al. Hplc assay for determination of amphotericin b in biological samples. Biomed Chromatogr. 2008;22(4):402–407. doi: 10.1002/bmc.947.

[18] Shahnaz G, Edagwa BJ, McMillan J, et al. Development of mannose-anchored thiolated amphotericin b nanocarriers for treatment of visceral leishmaniasis. Nanomedicine (Lond). 2017;12(2):99–115. doi: 10.2217/nnm-2016-0325.

[19] Segura M, Gottschalk M. Streptococcus suis interactions with the murine macrophage cell line j774: adhesion and cytotoxicity. Infect Immun. 2002;70(8):4312–4322. doi: 10.1128/IAI.70.8.4312-4322.2002.

[20] Osman NMM. ; 2021Toxicology and cellular interactions of polymer-based nanocarriers for pulmonary drug delivery. Liverpool John Moores University (United Kingdom),

[21] Nahar M, Jain NK. Preparation, characterization and evaluation of targeting potential of amphotericin b-loaded engineered plga nanoparticles. J. Pharm Res. 2009;26(12):2588–2598. doi: 10.1007/s11095-009-9973-4.

[22] Jain S, Jain N, Bhadra D, et al. Transdermal delivery of an analgesic agent using elastic liposomes: preparation, characterization and performance evaluation. Curr Drug Deliv. 2005;2(3):223–233. doi: 10.2174/1567201054368020.

[23] Kim AR, An HJ, Jang ES, et al. Preparation, physical characterization, and in vitro skin permeation of deformable liposomes

loaded with taxifolin and taxifolin tetraoctanoate. European Journal of Lipid Science Technology. 2019;121:1800501.

[24] Chávez-Fumagalli MA, Ribeiro TG, Castilho RO, et al. New delivery systems for amphotericin b applied to the improvement of leishmaniasis treatment. Rev Soc Bras Med Trop. 2015;48(3):235–242. doi: 10.1590/0037-8682-0138-2015.

[25] Kudarha RR, Sawant KK. Chondroitin sulfate conjugation facilitates tumor cell internalization of albumin nanoparticles for brain-targeted delivery of temozolomide via cd44 receptor-mediated targeting. Drug Deliv Transl Res. 2021;11(5):1994–2008. doi: 10.1007/s13346-020-00861-x.

[26] Khan SA, Schneider M. SPIE; 2013 Nanoprecipitation versus two step desolvation technique for the preparation of gelatin nanoparticles., PWB. doi: 10.1117/12.2002419.

[27] Pal D, Saha S. Chondroitin: a natural biomarker with immense biomedical applications. RSC Adv. 2019;9(48):28061–28077. doi: 10.1039/c9ra05546k.

[28] Leteux C, Chai W, Loveless RW, et al. The cysteine-rich domain of the macrophage mannose receptor is a multispecific lectin that recognizes chondroitin sulfates a and b and sulfated oligosaccharides of blood group lewisa and lewisx types in addition to the sulfated n-glycans of lutropin. J Exp Med. 2000;191(7):1117–1126. doi: 10.1084/jem.191.7.1117.

[29] Hoare DG, Koshland D.Jr. A procedure for the selective modification of carboxyl groups in proteins. J Am Chem Soc. 1966;88(9):2057–2058. doi: 10.1021/ja00961a045.

[30] Nègre E, Chance ML, Hanboula SY, et al. Antileishmanial drug targeting through glycosylated polymers specifically internalized by macrophage membrane lectins. Antimicrob Agents Chemother. 1992;36(10):2228–2232. doi: 10.1128/AAC.36.10.2228.

[31] Godwin DA, Michniak BB, Creek KE. Evaluation of transdermal penetration enhancers using a novel skin alternative. J Pharm Sci. 1997;86(9):1001–1005. doi: 10.1021/js9700457.